

2018

Estimation of Refrigerant Charge Inventory for an Automotive Air Conditioning System

Vikas Pulinkuzhi

Birla Institute of Technology and Science Pilani— Hyderabad Campus, 500078, India, h2016148056@hyderabad.bits-pilani.ac.in

Vatsal Thakor

Birla Institute of Technology and Science Pilani— Hyderabad Campus, 500078, India, h2016148052@hyderabad.bits-pilani.ac.in

Santanu Prasad Datta

Birla Institute of Technology & Science Pilani, Hyderabad Campus, India, spdatta@hyderabad.bits-pilani.ac.in

Prasanta Kumar Das

pkd@mech.iitkgp.ernet.in

Follow this and additional works at: <https://docs.lib.purdue.edu/iracc>

Pulinkuzhi, Vikas; Thakor, Vatsal; Datta, Santanu Prasad; and Das, Prasanta Kumar, "Estimation of Refrigerant Charge Inventory for an Automotive Air Conditioning System" (2018). *International Refrigeration and Air Conditioning Conference*. Paper 1945.
<https://docs.lib.purdue.edu/iracc/1945>

This document has been made available through Purdue e-Pubs, a service of the Purdue University Libraries. Please contact epubs@purdue.edu for additional information.

Complete proceedings may be acquired in print and on CD-ROM directly from the Ray W. Herrick Laboratories at <https://engineering.purdue.edu/Herrick/Events/orderlit.html>

Estimation of Refrigerant Charge Inventory for an Automotive Air Conditioning System

Vikas PULINKUZH¹, Vatsal THAKOR¹, Santanu P. DATTA^{*1}, Prasanta K. DAS²

¹Department of Mechanical Engineering,
Birla Institute of Technology and Science Pilani— Hyderabad Campus, 500078, India
h2016148056@hyderabad.bits-pilani.ac.in
h2016148052@hyderabad.bits-pilani.ac.in
spdatta@hyderabad.bits-pilani.ac.in

²Department of Mechanical Engineering,
Indian Institute of Technology Kharagpur, 721302, India
pkd@mech.iitkgp.ernet.in

* Corresponding Author

ABSTRACT

The knowledge about the refrigerant charge distribution in each component of an automotive air-conditioning system (AACS) is essential to predict any leakage into the system, health monitoring and estimation of overall system performances. However, estimating charge distribution in each component is not as easy as finding the total refrigerant mass into the system. It is observed mostly the condenser and the evaporator are the two major components, which consume maximum volume of refrigerant. In this present work the refrigerant inventory in each component of an AACS are estimated by using an analytical technique which is a modified version of Otaki method. It gives an advantage over actual Otaki method by ignoring the outside heat transfer coefficient to accommodate the design complexity of an automotive heat exchanger. Though the heat exchangers are the major stake holders of refrigerant, the residual refrigerant in compressor, liquid line, vapor line and expansion device is estimated according to their volume and density by this modified Otaki method. A comparative study between the Otaki and modified Otaki method justifies the acceptability of the later for a wide range of experimental data with the variation of compressor speed, blower speed and refrigerant charge from undercharging to overcharging.

1. INTRODUCTION

During the last few decades, research on Automotive Air Conditioning System (AACS) reached a milestone in terms of comfort, safety and economy. However, investigation on system performance due to AACS's variable operating conditions is limited. The inventory of a refrigeration system is the amount of refrigerant mass distributed among the components in the refrigeration equipment. Now the refrigerant charge inventory depends on the size of equipment, operating conditions and the thermodynamic state of the fluid inside the components.

The main focus is on the evaporator and the condenser, as phase change occurs in them, which makes their modelling difficult. Estimation of exact amount of refrigerant is essential to obtain the optimum performance of the system. There are many factors, which governs the distribution of refrigerant such as speed of compressor, blower speed and ambient temperature. Due to this, the refrigerant distribution in each component of an AACS is not uniform for a particular running condition. Further, the condenser and the evaporator are the two important components, which consume maximum volume of refrigerant. Porto et al. (2013) observed that the condenser and the discharge line would almost make 88 percent of the total refrigerant mass while the remaining refrigerant is distributed in all other components. As the charge varies, the system experience ranges from undercharging to overcharging as depicted in the T-s diagram shown in Figure 1.

Estimation of refrigerant charge in an AACS is vital for various reasons. Firstly, COP is affected with the refrigerant amount (Datta, Das, & Mukhopadhyay, 2013; Youbi-Idrissi, Macchi-Tejeda, Fournaison, & Guilpart, 2007), which indicates there is an optimal refrigerant charge amount needed for highest COP. There are also environmental reasons associated with the use of more refrigerants like (HCFCs, HFC) due to greenhouse effect. In addition, the compressor performance and service life is also affected. Further, the manufacturers mostly provide the specific mass to be used in the equipment. However, the system needs to be recharged (due to leakage) occasionally, and this requires estimating the current refrigerant charge distribution.

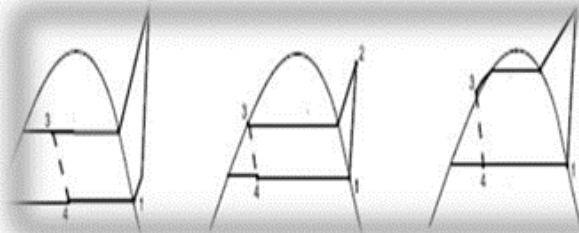


Figure 1: T-s diagram showing undercharge to overcharge (left to right)

Otaki (1971) developed a method to predict the mass inside a refrigerant system by employing an energy balance between the secondary fluid and the single-phase fluid in the heat exchangers. However, correlations for finding the heat transfer coefficients are critical to this approach, and can be usually obtained from the literature (Hughmark, 1965; Rice, 1987; Shah, 1982). The major limitation of Otaki method is its dependency on a known external heat transfer coefficient. These correlations are not much effective in case of complexed heat exchangers like louvered-fin automotive heat exchanger. Therefore, Porto et al. (2013) proposed a modified version of Otaki method to overcome the limitation of actual Otaki method (Otaki, 1971). In this modified Otaki model, the effect of external heat transfer coefficient of the secondary fluid can be ignored towards the estimation of the refrigerant mass distribution. The study validates this method successfully through experimental results and convergence test. In one of their experimental validation, it was noted that the condenser and liquid line contains 88% of the charge, which signifies the subcooled temperature as a vital state point. The influence of compressor speed also plays an important role on the refrigerant mass distribution in the evaporator and the condenser (Kaynaklı & Horuz, 2003). They also assessed that an increase in air inlet temperature increases both the cooling capacity and COP of the system.

Ratts and Brown (2000) investigated the thermodynamic losses in different components of a cycling clutch, orifice tube type AACCS through a combination of experiment and second law analysis for different car speeds. Hosoz and Direk (2006) have developed a stationary R134a based AACCS which can operate both on heat pump (air to air) and air conditioning modes. It was observed that the heat pump operation usually yielded a higher COP and a lower rate of exergy destruction. Qi et. al. (2007) have investigated a new displacement control for a variable displacement compressor in connection with an automotive air conditioning system.

Only limited efforts have been made for the theoretical analysis of automotive HVAC systems. Lee and Yoo (2000) developed a simulation program for an automotive air conditioning system to investigate the effect of condenser volume and the refrigerant charge quantity. It is reported that 10% overcharging resulted in the best performance of the system. In a similar kind of investigation, Jabardo et al. (2002) observed no effect of refrigerant charge on system performance as the contradiction to that of Lee and Yoo (2000). Hosoz and Ertunc (2006), Atik et al. (2007) and Kamar et al. (2013) used artificial neural network (ANN) to predict the performance of a stationary AACCS. Trzebiński & Szczygieł (2010) conducted a thermodynamic analysis of car air conditioning considering different cases like controlled and uncontrolled expansion valve as well as uncontrolled and externally controlled compressor. Effect of refrigerant charge and ambient temperature has also been studied.

From the above literature survey, it is understandable that there are limited investigation on the refrigerant inventory analysis till date. Particularly, investigation based on experimental observations are less with varying degree of accuracy. Therefore, in this paper, the mass distribution in each component considering phase change of refrigerant inside heat exchangers are estimated along with the corresponding phase lengths. This study was continued under several operating conditions to check the model accuracy. The modified Otaki method is also validated by steady-state measurements for an AACCS. The experimental results showed better agreement with the predictions from the Otaki method.

2. DEVELOPMENT OF THE EXPERIMENTAL FACILITY

There are some distinct differences between the AACCS and the conventional building or industrial refrigeration and air-conditioning system because of the compactness, capacity and highly variable operating conditions of the former. It has been decided to develop a stationary test facility (Figure 2) of an automotive air conditioning system by using all actual automotive components like the swash plate compressor, the microchannel heat exchangers and the thermostatic expansion valve (Table 1). Apart from these basic four components, the test rig has been equipped with some additional components like oil separator, filter/drier, sight glasses etc. As in case of the original AACCS, the developed test rig is also charged with R-134a. The swash plate compressor runs at different speeds as it is

driven by the engine in the car. In the test facility, instead of an engine a variable speed motor drive has been used to run the compressor via a multiple v-belt and a magnetic clutch. Separate ducting arrangement has been made for condenser and evaporator to facilitate monitoring and measurement of the air stream (both flow rate and temperature). The details of the system can be referred from Datta et al. (2013).

The parameters measured in this test system include the compressor and blower speeds, refrigerant mass flow rate using a Coriolis type mass flow meter (measurement uncertainties of $\pm 0.75\%$), the temperatures (measurement uncertainties of $\pm 0.5^\circ\text{C}$) and pressures (measurement uncertainties of $\pm 0.25\%$) of refrigerant at different strategic points of the refrigerant loop, the air flow rate (measurement uncertainties of $\pm 3.0\%$), dry-bulb temperatures and relative humidity at the heat exchangers inlet and outlet (measurement uncertainties of $\pm 2.0\%$).

The experiments are carried out with varying compressor and blower speed along with a variable refrigerant charge for a given ambient condition. Total sixty set of experiments are conducted at 200, 300, 400, 500 and 600 g of refrigerant charge level. In each charge level the speed of the compressor is fixed at 1000, 1300, 1600 and 1900 rpm by using the variable frequency drive. Again, for each compressor speed, the blower speed of the evaporator is manually selected from existing control knobs at three different set points of 2208, 3092 and 3475 rpm. Separate measurements are made to estimate the air flow rates corresponding to each of the blower speeds. They are 64, 78 and 88 m^3h^{-1} respectively. The air flow through the condenser is 1345.5 m^3h^{-1} . Typical test runs are repeated and a good reproducibility has been observed.

The maximum uncertainties (Moffat, 1988) of $\dot{Q}_{eva,ref}$, $\dot{W}_{comp,ref}$ and COP_{ref} at highest charge level are 1.75%, 1.76% and 4.72% respectively based on the accuracies of various measured variables discussed above.

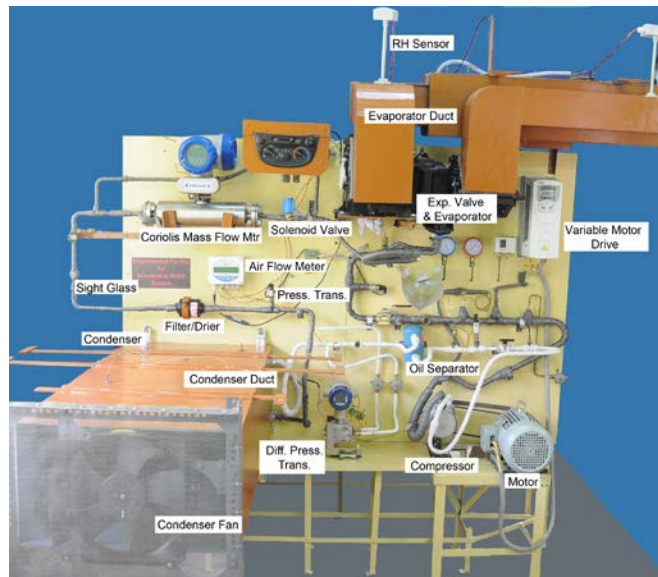


Figure 2: Photographic view of the test rig

Table 1: Details of the actual automotive HVAC components

Component	Description	Dimension/Specification
Evaporator	<ul style="list-style-type: none"> Multi-flow evaporator Fin tube type cross-flow exchanger 	Size: 240mm x 197mm x 48 mm Number of tubes: 19
Condenser	<ul style="list-style-type: none"> Multi-flow Condenser with fan cooling Fin tube type cross-flow exchanger Receiver coupled at the outlet of condenser for separating liquid refrigerants 	Size: 540mm x 480mm x 163.1 mm Number of tubes: 31 Number of passes: 4; with 14, 7, 6 and 4 tubes in 1 st , 2 nd , 3 rd and 4 th pass respectively
Compressor	<ul style="list-style-type: none"> Fixed displacement swash plate compressor with five pistons Designed to be driven by engine shaft through belt drive and magnetic clutch 	Type: SP08 Runs between: 800 to 2200 rpm Pressure Range: 100 to 1800 kpa
Expansion valve	Orifice type, thermostatically controlled	-

3. MODELING

In view of the above discussion, in this present work the refrigerant inventory in each component of an AACS are estimated by using ‘modified Otaki method’ (Porto et al., 2013). Further, the system performance and refrigerant charge distribution are also estimated under varying operating conditions from undercharge to overcharge. The entire system is divided into evaporator, condenser, high pressure and low pressure tubes and static components. As the compressor and the expansion valve are having fast dynamics and lesser volume, negligible amount of refrigerant inventory are considered in this study. The physical parameters like surface area, volume, etc. are calculated based on the available data from Table 1.

3.1 Method used to predict mass in a heat exchanger

The modified Otaki method solves the energy equation (or first law of thermodynamics) of the heat exchangers to obtain the lengths of different phase regions. As this method does not use external heat transfer coefficient in its modelling, it is preferred for an unconventional or complex heat exchanger like the AACS over ‘Otaki method’. The existence of single-phase and two-phase region in the evaporator and the condenser prompts the inventory calculation to involve different correlations for calculation of heat transfer coefficient and void fraction. A control volume is selected involving the refrigerant tubing for the superheated region, which allows us to find the energy balance between the refrigerant side and the water side (Figure 3). This depicts the use of first law of thermodynamics in Eqns. (1) - (4).

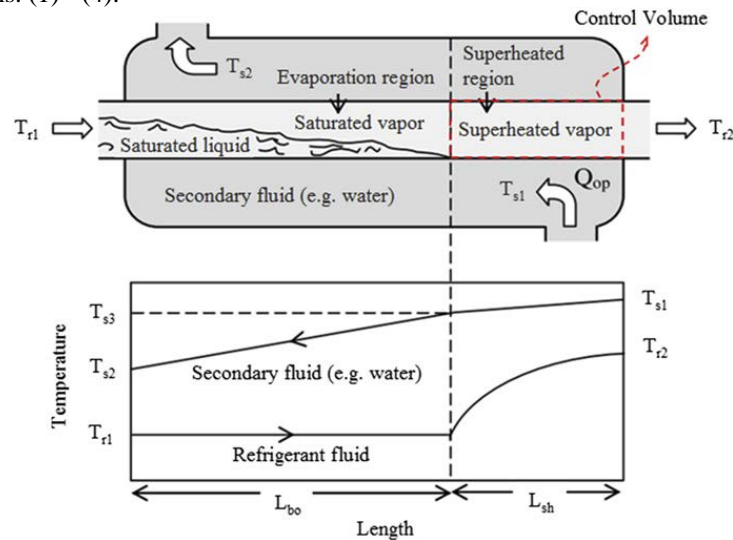


Figure 3. Counter-flow evaporator and temperature-length graph of the refrigerant and secondary fluid.

$$\dot{Q}_{sh} = \dot{m}_r \cdot (i_{r2} - i_{r3}) = \dot{m}_s \cdot c_{ps} \cdot (T_{s1} - T_{s3}) \quad (1)$$

$$\dot{Q}_{sh} = U_{sh} \cdot S_{sh} \cdot \Delta T_{sh} \quad (2)$$

$$U_{sh} = \left(\frac{1}{h_r} + R_w + \frac{1}{h_s \cdot R_s} \right) \quad (3)$$

$$\Delta T_{sh} = \frac{[(T_{s3} - T_{r1}) - (T_{s1} - T_{r2})]}{\ln \left[\frac{(T_{s3} - T_{r1})}{(T_{s1} - T_{r2})} \right]} \quad (4)$$

where Q_{sh} is the heat transfer rate from the air / secondary fluid to the refrigerant, m_s and C_{ps} are the mass flow and the specific heat of the secondary fluid, respectively, and m_r is the refrigerant mass flow. Further T_{s1} and T_{s3} are the

air fluid temperatures at the entrance and exit respectively while i_{r3} and i_{r2} are the enthalpies of refrigerant. R_s is the surface ratio (between the secondary surface area and the refrigerant surface area). S_{sh} and ΔT_{sh} are the heat transfer surface area and the LMTD, respectively. U_{sh} is the overall heat transfer coefficient, which is a function of h_r (heat transfer coefficients of the refrigerant) and h_s (heat transfer coefficients of the air) while R_w is the wall thermal resistance.

Modified Otaki method is based on algebraic system of two equations and two unknowns. The unknowns are surface area of the superheated region (S_{sh}), and heat transfer coefficient on the secondary side (h_s, R_s). The first equation is the energy equation of superheat zone. The second equation is obtained by applying the energy balance to the two-phase region which can be done similarly as shown earlier. It is important to observe that the term h_s, R_s is considered constant in the super-heated and two-phase regions, due to which we can be able to solve the equation simultaneously.

The analysis starts with finding the two-phase and the single-phase lengths which are used to calculate the mass in the heat exchanges. The refrigerant charge in compressor, liquid line, vapour line and expansion valve are calculated according to their volume and density. The model calculates the interface temperature between phase boundary, which facilitates in calculating the length of single and two-phase flow region.

The following correlations have been used in this modelling:

- Shah correlation for condensing heat transfer coefficient, (Shah, 1982)
- Dittus-Boelter correlation for heat transfer coefficient of refrigerant in single-phase region, (Dittus & Boelter, 1985)
- Lockhart-Martinelli correlation for heat transfer coefficient of refrigerant in two-phase region, (Lockhart & Martinelli, 1949)
- Addoms correlation for boiling heat transfer coefficient, and (Shah, 1982)
- Hughmarks correlation for estimating void fraction (Hughmark, 1965)

Based on the above equations and correlations, the heat transfer in boiling and heat transfer rate in superheated condition are calculated. In addition, the LMTD for both the two-phase and boiling region are calculated for the ease of operation. All the above results help in determining the surface area of superheated region from simultaneously solving energy equation for both the regions. Superheated length is obtained from the superheated area. This concludes the first section of the algorithm of finding the superheated length of evaporator tubes. The next section involves finding the mass of two-phase region which is only possible through determining the void fraction of two-phase which keeps changing along the two-phase length of evaporator tubes. Thus, as the quality changes from 0.3 to 1 (for case of 500-gram refrigerant), there is change of void fraction which also moves towards 'one' non-linearly. There is a need to iterate to calculate the void fraction from correlation.

$$\alpha_{\text{hom}} = \frac{1}{\left[1 + \frac{\rho_v \cdot (1 - x)}{\rho_l \cdot x}\right]} \quad (5)$$

$$\alpha = K \cdot \alpha_{\text{hom}} \quad (6)$$

$$Z = \left[\frac{d \cdot G}{\mu_l + \alpha \cdot (\mu_v - \mu_l)} \right]^{1/6} \cdot \left\{ \frac{1}{g \cdot d} \cdot \left[\frac{G \cdot x}{\rho_v \cdot \alpha_{\text{hom}} \cdot (1 - \alpha_{\text{hom}})} \right]^2 \right\}^{1/8} \quad (7)$$

The above equations are part of Hughmark's correlation for determining void fraction where parameters like density of liquid and gaseous refrigerant, quality, mass flux, diameter, viscosity of liquid and gaseous refrigerant are used. The k values in the above relation is obtained from data below.

Table 2: K-value Table

Z	1.3	1.5	2	3	4	5	6	7	10
K	0.185	0.225	0.325	0.49	0.605	0.675	0.720	0.76	0.78

The basic objective of finding the void fraction was to use it to find the average refrigerant density of two-phase region which is calculated as:

$$\rho_r = \rho_l \cdot (1 - \alpha) + \alpha \cdot \rho_v \quad (8)$$

The next step is to find the two-phase mass or boiling mass:

$$M_{bo} = \sum (\rho_r \cdot \Delta V) \quad (9)$$

The evaporation refrigerant mass is just the sum of two-phase mass and the superheat mass. This concludes the modelling of evaporator. Modelling of condenser is very similar to that of evaporator. There is additional phase in condenser. The three phases of condenser are as follows:

- Superheated phase
- Two-phase/condensation phase
- Subcooled phase

To apply the modified Otaki method for a condenser, the energy balance should be applied in the superheated vapour, condensation regions and sub-cooled liquid. The unknowns in the problem are the surface area / length of the single-phase flow regions and the secondary fluid heat transfer coefficient. Finally, the refrigerant masses in all the three regions are calculated using the same methodology applied to the evaporator.

This model is used to estimate the refrigerant distribution for different mass. The results from these analyses are to be clubbed with experimental results of Datta et al. (2013) to get a more comprehensive understanding of the distribution of the refrigerant mass charge in an AACS. There are some inherent inputs to be given in the simulation such as properties of refrigerant (R134a) and air which is obtained by interfacing the MATLAB software with REFPROP software. Other inputs like temperature and enthalpies at various states are also extracted from REFPROP.

4. RESULTS AND DISCUSSION

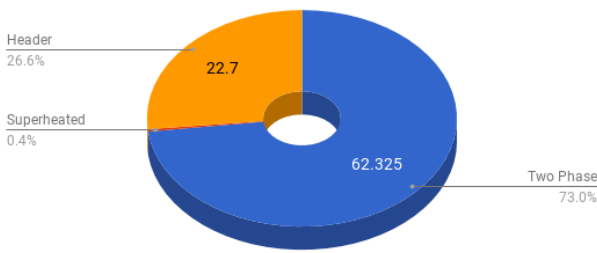
The actual thermal-hydraulic process followed by a system is immensely useful for understanding as well as assessing the system performance. On the other hand, the representation of any practical refrigeration cycle purely based on parametric measurements could be difficult as there are auxiliary components and connecting pipelines. Further, due to the physical constraints, any system will have only a limited number of measurement stations with conventional sensors (mainly for pressure and temperature). The present test rig is also not free from these limitations. Nevertheless, a simplified representation of the thermodynamic cycle followed by the system is possible based on some common assumptions such as no pressure drop across the heat exchangers and secondly, any effect of tube bends, connectors and valves has also been ignored. The effect of refrigerant charge, compressor speed and blower speed on the system performance and corresponding refrigerant distribution in each component are discussed below.

4.1 Effect of refrigerant charge

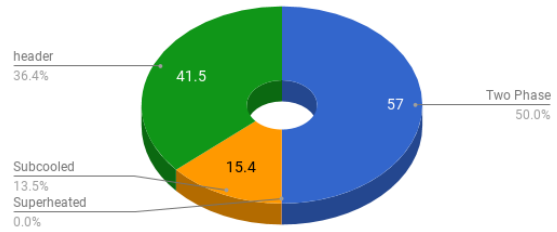
Both the heat exchangers of the AACS are two major components, which consume maximum refrigerant charge. The refrigerant charge distribution inside the evaporator and the condenser are estimated using Eqs (1-9) based on available experimental data at 500g refrigerant charge input and 1600 rpm compressor speed with blower settings of Set 3. Figure 4 shows high charge concentration in the header and the two-phase region of both the heat exchangers, which is predictable due to the higher density of refrigerant at those particular regions. As the receiver is an integrated part of any automotive heat exchanger, they consume a large amount of refrigerant for uninterrupted flow phenomena. From Fig. 4b, it is understandable that the condenser is oversized and having higher heat transfer coefficient which can easily overcome the region of superheat within fraction of its total length.

In addition to the above investigation, the refrigerant charge distribution in each component of the AACS are shown in Fig. 5 for the same operating conditions. It may be noted that the refrigerant accumulation in the compressor and the expansion device are negligible comparing to the other components due to their first dynamics and lesser volume. As the test rig is customized to accommodate a large number of measuring and auxiliary equipment, the length of suction and discharge line increases up to a certain level. Owing to this, significant amount of refrigerant accumulation is observed in both the high and low pressure lines.

EVAPORER MASS DISTRIBUTION



CONDENSER CHARGE DISTRIBUTION



(a)

(b)

Figure 4: Refrigerant charge distribution using modified Otaki method in (a) condenser, and (b) evaporator (at 500g refrigerant charge input and 1600 rpm compressor speed with blower settings of Set 3)

AACS CHARGE DISTRIBUTION

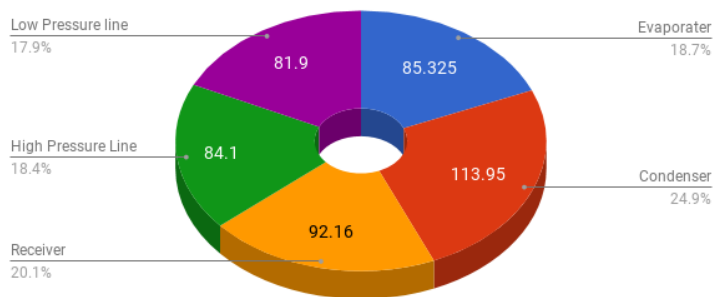


Figure 5: Refrigerant charge distribution using modified Otaki method in each component of an AACS at 500g refrigerant charge input and 1600 rpm compressor speed with blower settings of Set 3

In Figure 6, the refrigerant charge distribution in each component is presented from undercharging to overcharging of the system. Both these phenomena are not desirable for the operation of an AACS. The undercharge, which indicates leakage into the system, leads to compressor heating and less cooling. Similarly, the overcharge leads to flooding of the heat exchangers, which results certain choking phenomena inside the system. From Figure 6, it is understandable that with the increase of refrigerant charge, accumulation of refrigerant inside the evaporator and the condenser also increases.

REFRIGERANT DISTRIBUTION FOR DIFFERENT INPUT CHARGES

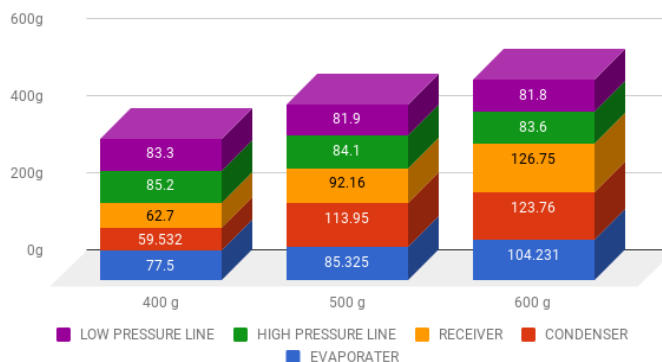


Figure 6: Distribution of refrigerant charge using modified Otaki method in each component of an AACS from undercharging to overcharging

4.2 Effect of compressor speed

The effect of compressor speed on the refrigerant charge distribution in each component are reported in Figure 7 at a constant refrigerant charge level of 500 g. It is observed that the total refrigerant distribution in each component is almost constant at any compressor speed. However, the single phase and two phase lengths are varying with the increase of compressor speed. It indicates that with compressor speed refrigerant mass flow rate increases which affect the heat transfer phenomena of both the heat exchangers. Due to this, the length of superheated and subcooled zones of the condenser increases with compressor speed, whereas the opposite phenomena is observed in case of two phase length. Similarly, with the increase of compressor speed, the load into the system also increases which extends the two-phase length of the evaporator and decrease the superheated length.

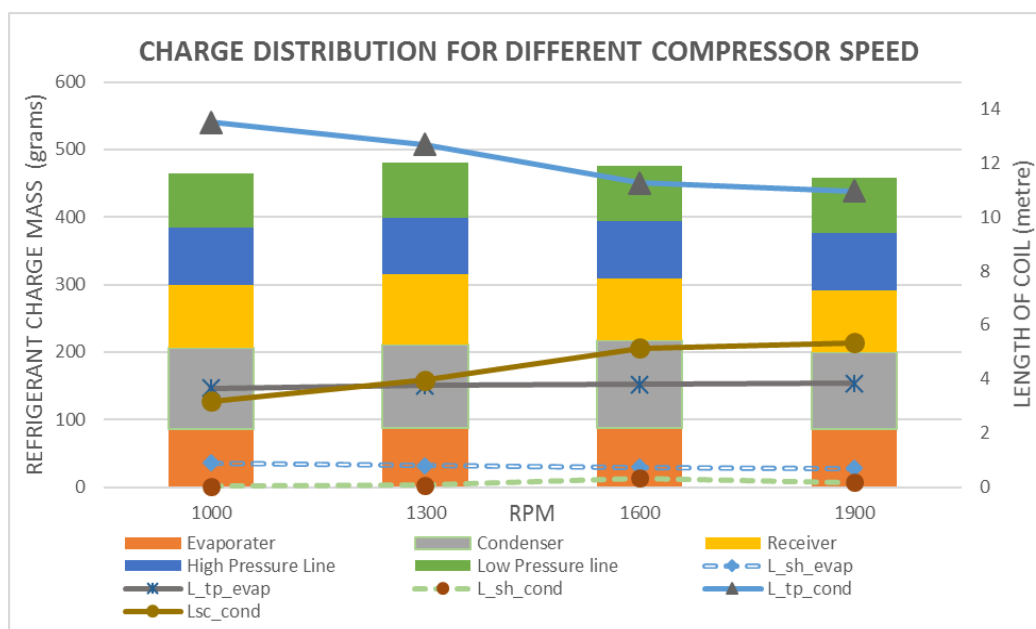


Figure 7: Effect of compressor speed on the refrigerant charge distribution using modified Otaki method in each component of an AACs

4.3 Effect of blower speed and overall system performance

A significant effect of blower speed is observed on the condenser performance due to the variation of load into the system (Figure 8). The condenser two phase length decreases with blower speed, whereas superheated and subcooled lengths increases with the same.

The cooling capacity increases both with the increase in compressor and blower speeds, though the effect of blower speed is not as pronounced as it is in the case of compressor speed (Figure 8). The increase in mass flow rate with compressor speed also enhances the cooling capacity. Similarly, compression work increases both with the compressor speed and refrigerant charge. As with the increase of speed and charge level, mass flow rate and the pressure ratio of the compressor increases, its direct consequences can be felt as the increase in compressor speed. So, the combined effect of these two parameters gives a substantial rise in compression work. As COP is the ratio of cooling capacity to compression work, increase of refrigerant charge and blower speed is expected to increase COP considerably as the pattern of cooling capacity.

4.4 Convergence Study

This method requires dividing the two-phase region into n number of parts. The increasing number of divisions would help in getting a refined system modelling and an accurate result with an expense of higher computational resources and time. Thus, we conducted the study to check the results with varying level of refinement for both the evaporator and the condenser. Both results show the variation in mass with refinement. It could be concluded that refinement after a stage would not bring about drastic change in the result. Thus, for saving time, one could go for lower refinement based on the time and computational capability, but on the expense of lower accuracy. Utmost care should be taken to maintain a minimum division (13 and 19 in this case) for reasonable accuracy.

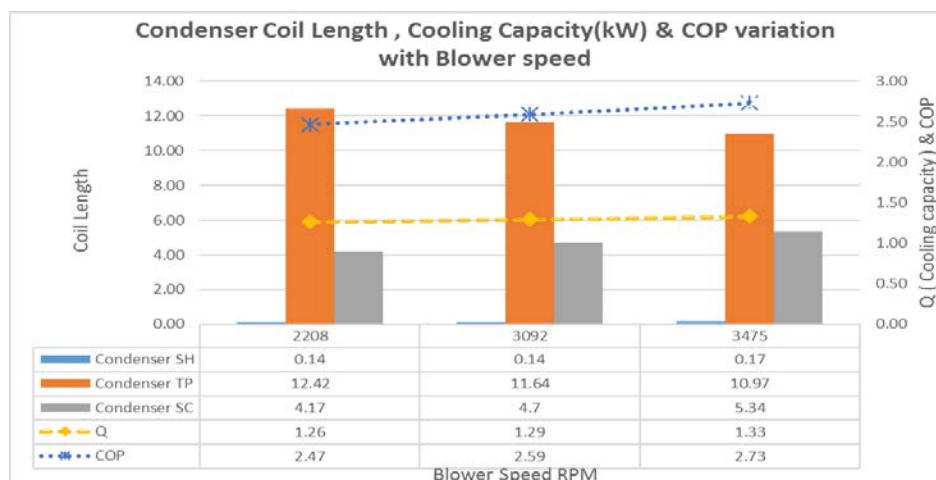


Figure 8: Effect of blower speed on the refrigerant charge distribution using modified Otaki method in condenser and variation of overall system performance

4. CONCLUSIONS

A stationary test bench has been developed for the investigation of steady state and dynamic performance of an automotive air conditioning system. The test facility replicates the hardware arrangement of the actual automobile as far as practicable and uses the components used in the actual system. As the engine is absent in the facility the variation of the compressor speed is achieved through a variable frequency motor which engages with the compressor through a magnetic clutch. The facility also contains a large number of sensors in excess to those few present in the actual system. The steady state performance of the system has been investigated for three independent variables, namely the refrigerant charge level, the compressor speed and the speed of the evaporator fan as they are the only variable parameters for a running car. The following trends have been observed.

- The refrigerant mass distribution in each component of an AACS is efficiently estimated by modified Otaki method. The total 90% accumulation of refrigerant mass is observed for any given charge condition. It indicates the proficiency of modified Otaki method comparing to actual Otaki method.
- From this model, both the two phase and single phase lengths of the heat exchangers are correctly identified.
- In any case, maximum charge accumulation is observed in both the heat exchangers along with the receiver/ accumulator and the pipelines.
- With the increase of compressor speed, cooling load and compression work increases whereas, COP of system decreases.
- With the increase of refrigerant charge cooling capacity and COP of the system increases up to a certain range then, it decreases whereas, the compression work continuously increases with the refrigerant charge.

NOMENCLATURE

d	inner diameter	G	mass flux
h	heat transfer coefficient		
i	enthalpy		
K	Hughmark correlation factor	m	mass flow
Q	heat transfer rate		
R_w	heat exchanger wall resistance	R_s	surface ratio
S	surface area		
U	global heat transfer coefficient		
\times	quality		
Z	Hughmark correlation parameter		
α	void fraction		
\dot{X}	Martinelli parameter		

REFERENCES

- Datta, S. P., Das, P. K., & Mukhopadhyay, S. (2013). Performance of an automotive airconditioning test rig with restricted air flow through the condenser. In *Proceedings of the 22th National and 11th International ISHMT-ASME Heat and Mass Transfer Conference*. IIT Kharagpur, Kharagpur, India.
- Dittus, F. W., & Boelter, L. M. K. (1985). Heat transfer in automobile radiators of the tubular type. *International Communications in Heat and Mass Transfer*, 12(1), 3–22. [http://doi.org/10.1016/0735-1933\(85\)90003-X](http://doi.org/10.1016/0735-1933(85)90003-X)
- Hosoz, M., & Direk, M. (2006). Performance evaluation of an integrated automotive air conditioning and heat pump system. *Energy Conversion and Management*, 47, 545–559. <http://doi.org/10.1016/j.enconman.2005.05.004>
- Hosoz, M., & Ertunc, H. M. (2006). Artificial neural network analysis of an automobile air conditioning system. *Energy Conversion and Management*, 47(11-12), 1574–1587. <http://doi.org/10.1016/j.enconman.2005.08.008>
- Hughmark, G. A. (1965). Holdup and heat transfer in horizontal slug gas-liquid flow. *Chemical Engineering Science*, 20(12), 1007–1010. [http://doi.org/10.1016/0009-2509\(65\)80101-4](http://doi.org/10.1016/0009-2509(65)80101-4)
- Jabardo, J. M. S., Mamani, W. G., & Ianella, M. R. (2002). Modeling experimental evaluation of an automotive air conditioning system with a variable capacity compressor. *International Journal of Refrigeration*, 25, 1157–1172. [http://doi.org/10.1016/S0140-7007\(02\)00002-6](http://doi.org/10.1016/S0140-7007(02)00002-6)
- Kamar, H. M., Ahmad, R., Kamsah, N. B., & Mohamad Mustafa, A. F. (2013). Artificial neural networks for automotive air-conditioning systems performance prediction. *Applied Thermal Engineering*, 50(1), 63–70. <http://doi.org/10.1016/j.applthermaleng.2012.05.032>
- Kaynaklı, Ö., & Horuz, I. (2003). An experimental analysis of automotive air conditioning system. *International Communications in Heat and Mass Transfer*, 30(2), 273–284.
- Lee, G. H., & Yoo, J. Y. (2000). Performance analysis and simulation of automobile air conditioning system. *International Journal of Refrigeration*, 23, 243–254. [http://doi.org/10.1016/S0140-7007\(99\)00047-X](http://doi.org/10.1016/S0140-7007(99)00047-X)
- Lockhart, R., & Martinelli, R. (1949). Proposed correlation of data for isothermal two-phase, two-component flow in pipes. *Chemical Engineering Progress*, 45(1), 39–48.
- Moffat, R. J. (1988). Describing the uncertainties in experimental results. *Experimental Thermal and Fluid Science*, 1, 3–17. [http://doi.org/10.1016/0894-1777\(88\)90043-X](http://doi.org/10.1016/0894-1777(88)90043-X)
- Otaki, T. (1971). Holding refrigerant in refrigeration unit. Prog. Refrigeration Sci. Technol. In *Proceedings of the XIII International Congress of Refrigeration* (pp. 535–544). AVI Publishing Company, Inc., Washington, DC.
- Porto, M. P., Koury, R. N. N., & Machado, L. (2013). An alternative method to estimate refrigeration system inventory. *Applied Thermal Engineering*, 52(2), 313–320. <http://doi.org/10.1016/j.applthermaleng.2012.12.023>
- Qi, Z. G., Chen, J. P., Chen, Z. J., Hu, W., & He, B. (2007). Experimental study of an auto-controlled automobile air conditioning system with an externally-controlled variable displacement compressor. *Applied Thermal Engineering*, 27, 927–933. <http://doi.org/10.1016/j.applthermaleng.2006.08.017>
- Ratts, E. B., & Brown, J. S. (2000). An experimental analysis of cycling in an automotive air conditioning system. *Applied Thermal Engineering*, 20, 1039–1058. [http://doi.org/10.1016/S0735-1933\(03\)00038-1](http://doi.org/10.1016/S0735-1933(03)00038-1)
- Rice, C. K. (1987). Effect of Void Fraction Correlation and Heat Flux Assumption on Refrigerant Charge Inventory Predictions. *ASHRAE Transactions*, 93(3035), 341–367.
- Shah, M. M. (1982). Chart Correlation for Saturated Boiling Heat Transfer: Equations and Further Study. *ASHRAE Transactions*.
- Trzebiński, D., & Szczygieł, I. (2010). Thermal analysis of car air conditioning. *Archives of Thermodynamics*, 31(4), 71–80. <http://doi.org/10.2478/v10173-010-0029-2>
- Yilmaz, S., & Atik, K. (2007). Modeling of a mechanical cooling system with variable cooling capacity by using artificial neural network. *Applied Thermal Engineering*, 27(13), 2308–2313. <http://doi.org/10.1016/j.applthermaleng.2007.01.030>
- Youbi-Idrissi, M., Macchi-Tejeda, H., Fournaison, L., & Guilpart, J. (2007). Numerical model of sprayed air cooled condenser coupled to refrigerating system. *Energy Conversion and Management*, 48(7), 1943–1951. <http://doi.org/10.1016/j.enconman.2007.01.025>